Physical Modeling of Atmospheric Transport of Stack Emissions at Kahe Electrical Generating Plant, Oahu, Hawaii

VOLUME I

by

J. E. Cermak* and D. G. Mutter**

Prepared for

Stearns-Roger, Inc.
Denver, Colorado

Fluid Dynamics and Diffusion Laboratory
Fluid Mechanics and Wind Engineering Program
Colorado State University
Ft. Collins, Colorado 80523

April 3, 1978 CER77-78JEC-DGM28a

*Director, Fluid Dynamics and Diffusion Laboratory
**Graduate Research Assistant, Department of Civil Engineering

ABSTRACT

Two models, with scales of 1:6000 and 1:650, of the Kahe Electrical Generating Plant (located on the island of Oahu, Hawaii) were tested in a wind tunnel in order to determine the nature of atmospheric transport of stack emissions. The heights and configuration of the stacks were varied as were wind velocity and direction. Ground-level concentrations of tracer gas were measured for each combination of conditions. Plume geometry and behavior were observed and recorded by means of still photographs, movies and videotape.

ACKNOWLEDGMENTS

Stearns-Roger, Inc. provided the 1:6000 scale model used in the first phase of the study. The 1:650 scale model was constructed at Colorado State University under the supervision of J. A. Garrison. R. L. Petersen was responsible for initial project organization.

The gas-tracer analyses were performed by J. Maxton and K. Cary, velocity measurements were made by H. Woo, S. Ayad, and J. J. Lou. J. A. Garrison, J. Hurd, and C. Powell were responsible for project photography.

TABLE OF CONTENTS

VOLUME I

*Color motion pictures, black and white photographs and color transparencies of plume behavior are provided, as a record of this investigation, apart from this report.

LIST OF FIGURES

Figure		Page

LIST OF TABLES

LIST OF SYMBOLS

Symbol	Definition	Dimensions
B	Maximum dimension of KEGP complex	(L)
D	Stack diameter	(L)
Fr	Froude number $\frac{V^2}{g(\frac{\Delta\rho}{\rho_a})D}$	(-)
g	Gravitational constant	(L/T^2)
H	Stack height	(L)
K	Concentration coefficient $\frac{\chi V_a D^2}{Q_s}$	(-)
Q_s	Source strength	(M/T)
R	Exhaust velocity ratio V_s/V_a	(-)
Re	Reynolds number $\frac{V_s B}{\nu}$	(-)
V	Mean velocity	(L/T)
z_o	Surface roughness	(L)

Symbol	Definition	Dimensions
(Greek Symbols)		
χ	Local concentration	(M/L^3 or ppm)
ν	Kinematic viscosity	(L^2/T)
δ	Boundary-layer thickness	(L)
γ	Specific weight	(M/T^2L^2)
ρ	Density	(M/L^3)
Ω	Angular velocity	(1/L)
μ	Dynamic viscosity	M/(TL)
(Subscripts)		
a	Meteorological tower	
s	Stack	
m	Model	
p	Prototype	
max	Maximum	
g	Geostrophic or gradient wind	
rms	Root-mean-square	
o	Reference value	

CONVERSION TABLE

(English to Metric Units)

Multiply Units	by	To Obtain
inches	2.540	centimeters
square inches	6.452	square centimeters
cubic inches	16.39	cubic centimeters
feet	0.3048	meters
square feet	0.0929	square meters
cubic feet	0.02832	cubic meters
feet/second	0.3048	meters/second
miles/hour	0.4470	meters/second
cubic feet/minute	0.02832	cubic meters/minute
cubic feet/minute	0.00047	cubic meters/second

1. INTRODUCTION

Hawaiian Electric Company, Inc. operates a power generating facility, on the island of Oahu, which is known as the Kahe Electrical Generating Plant (KEGP). The plant is located west of Honolulu and adjacent to the ocean (see Figure 1). Five generating units are presently in operation and three additional units have been proposed for future development.

The purpose of this study was to determine ground-level concentrations of sulfur dioxide emanating from the existing and proposed units of the KEGP. This was accomplished through the use of two scale models and the environmental wind tunnel facility at Colorado State University. A 1:6000 scale model was employed to determine the relationship between wind patterns in Kahe bowl (near the plant site) and those over the Waianae mountain range which lies to the north and east. Subsequently, a test plan was designed for a 1:650 model of the KEGP and its local surroundings. For selected directions of gradient wind, the atmospheric transport of stack emissions in the vicinity of the KEGP was investigated. Concentrations of tracer gas (simulating sulfur dioxide releases at the plant site) were sampled over the model surface. Overall plume geometry and behavior were observed, and recorded by photographing smoke released at the plant site.

The results of the concentration measurements for all test runs have been tabulated in Appendix A (under separate cover--Volume II). Appendix B (under separate cover--Volume III) contains figures presenting isopleths of ground-level concentration resulting from emissions from individual stacks. Color motion pictures, color videotape, and still photographs were utilized to record plume behavior, and are on file at Colorado State University and Stearns-Roger, Inc.

2. SIMULATION OF ATMOSPHERIC MOTION

Wind tunnel simulation of atmospheric gas diffusion is predicated on the similarity between the wind tunnel and atmospheric boundary layers. The criteria for the required similarity have a physical basis in terms of the conservation of mass, momentum and energy. These basic criteria have been discussed in detail by Halitsky (1963), Martin (1965), Cermak (1966), and Lord et al. (1970). The model laws may be divided into requirements for geometric, dynamic, kinematic and thermic similarity. In addition, model and prototype similarity of upwind flow characteristics and surface boundary conditions is required.

When interest is focused on the vertical motion of plumes of heated gases emitted from stacks into a thermally neutral atmosphere, the following variables are of primary significance:

g = gravitational acceleration

ρ_a = density of ambient air

$\Delta\gamma = (\rho_a - \rho_s)g$ = difference in specific weight of ambient air and stack gas

Ω = local angular velocity component of the earth

μ_a = dynamic viscosity of ambient air

V_a = velocity of ambient wind at the meteorological station

V_s = exit velocity of stack gas

B = maximum dimension of building complex

H = stack height

D = stack diameter

δ_a = thickness of planetary boundary layer

z_o = roughness height for upwind surface

Grouping the independent variables into dimensionless parameters with

ρ_a, V_a and H as reference variables yields the following parameters upon which the dependent quantities of interest must depend:

$$\frac{\delta_a}{H}, \frac{z_o}{H}, \frac{D}{H}, \frac{B}{H}, \frac{V_a}{H\Omega}, \frac{V_s \rho_a B}{\mu_a}, \frac{V_s}{V_a}, \frac{\rho_a V_s^2}{\Delta\gamma D}, \frac{\Delta\gamma}{\rho g}$$

The boundary-layer-thickness parameter $\frac{\delta_a}{H}$ was estimated to be nearly equal for model and prototype. Near equality of the surface-roughness parameter $\frac{z_o}{H}$ for model and prototype was achieved through geometrical scaling of the KEGP stacks and upwind roughness. The stack and building geometry parameters $\frac{D}{H}$ and $\frac{B}{H}$ were equal for model and prototype.

Dynamic similarity is achieved in a strict sense if the Reynolds number, $\frac{V_s \rho_a B}{\mu_a}$, and the Rossby number, $\frac{V_a}{H\Omega}$, for the model are equal to their respective counterparts in the atmosphere. The model and prototype Rossby numbers cannot be made equal; however, over the short distances of interest in this study (approximately 2000 m) the Coriolis acceleration has little influence upon the flow. According to standard practice (Cermak, 1971), the requirement of equal Rossby numbers was therefore relaxed. The Reynolds number also cannot be made equal for the model and prototype. However, similarity is assured if the model Reynolds number exceeds a minimum value in the range from 3,300 to 11,000.

The velocity ratio $\frac{V_s}{V_a}$ was maintained equal in model and prototype for the various approach-flow velocities and stack configurations and exit velocities tested. The stack Froude number, $\frac{V_s^2 \rho_a}{\Delta\gamma D}$, was made equivalent in model and prototype by adding helium to the modeled stack gas in order to obtain an appropriately large value of $\Delta\gamma$.

In summary, the following criteria were adopted to ensure similarity between the modeled and atmospheric boundary layers:

1. $Fr_m = Fr_p$, $Fr = \dfrac{V_s^2 \rho_a}{\Delta\gamma D}$;

2. $R_m = R_p$, $R = \dfrac{V_s}{V_a}$;

3. $R_e > 3300$, $R_e = \dfrac{V_s \rho_a B}{\mu_a}$;

4. $z_{o_m} = z_{o_p}$;

5. geometric similarity

Table 2-1 summarizes the values of pertinent parameters for this study.

Given that similarity of atmospheric motion was achieved, the dimensionless parameter $\dfrac{\chi V_a D^2}{Q_s}$ (where χ is the concentration of stack emission at some point of interest, and Q_s is the source flow rate expressed by volume per unit time) was equivalent for model and prototype (Cermak et al., 1966; Halitsky, 1963).

3. EXPERIMENTAL APPARATUS AND PROCEDURE

3.1 Wind Tunnel

Figure 3.1 provides a schematic representation of the Environmental Wind Tunnel (EWT) which was used for this neutral thermal stratification case. This wind tunnel, which was designed especially for the study of atmospheric flow phenomena, incorporates such features as an adjustable ceiling (to allow the elimination of any longitudinal pressure gradients), rotating turntables for the adjustment of model orientation, transparent boundary walls, and a test section of sufficient length to permit reproduction of micro-meteorological behavior. Mean wind velocities of 0.06 to 37 m/s (0.14 to 80 mph) can be obtained in the EWT. With the use of vortex generators at the test-section entrance, boundary layers 4 feet thick can be obtained over the last 12 meters of the test section.

3.2 Models

3.2.1 1:6000 Scale Model

For the purpose of determining the relationship between the flow patterns in the near-vicinity of the KEGP and those over the Waianae Range, a 1:6000 scale model was employed. This model, which was constructed by Stearns-Roger Inc., was machined from high-density styrofoam and provided an accurate representation of the topography with a circle centered roughly over Mauna Kapu with an approximate diameter of 22 km (see Figure 1). Figure 3.2 shows the 1:6000 scale model in the wind tunnel; the flow is toward the reader and represents the 45° gradient wind direction. Figure 3.3 provides an outside view of the model near the entrance to the test section; the instruments employed for velocity measurement are visible in the foreground.

3.2.2 1:650 Scale Model

A 1:650 scale model was utilized in the study of plume dispersion near the KEGP site. This model was of laminated styrofoam construction and included machined facsimiles of all significant plant buildings and structures (Figure 3.4 shows a close-up view of the modeled plant site). Laminations were not smoothed in order that the model surface would be sufficiently rough that a laminar sublayer would not form and thus Reynolds-number independence would be assured. The 1:650 scale model was constructed in strips, of approximately 2.5 km width in prototype dimensions, aligned along the axes of six gradient-wind directions of particular interest(see Figure 1).

3.3 Flow Visualization

3.3.1 1:6000 Scale Model

Flow visualization for the 1:6000 scale model consisted of the observation of surface wind direction at various points of interest (in and near the Kahe bowl, in particular) with a selected gradient wind direction imposed. Surface wind patterns were determined by means of observing the movement of smoke releases (from passive point sources at the KEGP site and nearby meteorological station sites) and the positions of miniature wind vanes installed on the model surface. Figure 3.5 shows an array of vanes covering the Kahe bowl area.

The movement of smoke releases, and the position and directional stability of the wind vanes were recorded with a color motion-picture camera. Section 4.1 presents a listing of tests recorded on motion-picture film. Still pictures were taken to provide an additional record of the wind vane positions. The results of this phase of the model study were reviewed and a suitable test program was designed for the close-up (1:650 scale) model.

3.3.2 1:650 Scale Model

In order to define plume geometry and behavior, smoke was released from the modeled KEGP complex under controlled conditions and permanent records of its movement were made in the form of color motion pictures, color videotape and still pictures. Titanium tetrachloride was introduced into the stack effluent (which was modeled as to its properties and discharge rate) in order to produce a visible smoke.

Wind velocity and direction, stack height, and the number, operating level and position of generating units were varied during the flow-visualization tests. Table 4.1 presents a listing of the sequence of flow visualizations recorded on motion-picture film.

3.4 Effluent Dispersion Measurements

In order to determine the effects of the approach flow and plant configuration and operating level on the downwind distribution of effluent concentration, tracer gas(es) were released from the modeled stacks and ground-level air samples were collected at each of a grid of sample points located in the downwind direction (Figure 3.6 indicates the sample locations for each wind direction tested). Up to 35 samples per test were simultaneously withdrawn through small tubes projecting through the model to its surface. The time required for the samples to be withdrawn corresponded to approximately one hour in prototype dimensions. Subsequently, the sample-point concentrations of tracer gas(es) were determined by means of gas chromatography techniques. Methane, ethane, propane and butane were employed as tracer gases which were mixed with helium and nitrogen such that the properties (notably the buoyancy) and the discharge rate of the prototype stack effluent were properly simulated.

3.5 Velocity Measurements

Vertical profiles of velocity were measured on both models to determine their surface roughness (and hence ensure Reynolds-number independence) and to provide correlation with historical wind velocities recorded at nearby meteorological stations (Mauna Kapu, Barbers Point and Makakilo). Velocities were measured by means of hot-wire anemometry techniques.

4. TEST PROGRAM AND RESULTS

4.1 1:6000 Scale Model

Six gradient wind directions (0°, 72°, 153°, 180°, 243° and 333° azimuth) were initially selected for study due to their historical frequency of occurrence and/or due to the potential seriousness of their occurrence (with regard to plume dispersion effects). Subsequently, three additional wind directions (45°, 62° and 79°) were imposed in order to determine the sensitivity of the Kahe-area wind patterns to moderate changes in direction from that of the northeast trade winds.

4.2 1:650 Scale Model

Flow visualization and concentration measurement tests were carried out for various combinations of KEGP development (as affected by the addition of proposed generating units), stack height and exit velocity, and wind velocity and direction. Tables 4.1 and 4.2 summarize the test parameters for flow visualization and concentration measurement phases, respectively, utilizing the 1:650 scale model.

It should be noted that from two to four tracer gases were employed in each run listed in Table 4.2 (one tracer gas for stacks 1-4 and one each for stacks 1c, 5, 6, 7 and 8). As the gas chromatograph was capable of distinguishing between gases, each run accounts for the effects of the operation of from two to four individual stacks.

4.3 Results of Flow Visualization

4.3.1 1:6000 Scale Model

The ground-level wind patterns (as indicated by wind-vane positions) corresponding to each of the imposed gradient wind directions are presented in Figures 4.1 to 4.9. Gradient-wind speed in the wind tunnel was 2.1 m/s. The occurrence of separation and horizontal vortex formation are indicated symbolically by a small helix; the approximate location of flow reattachment is also indicated. Additional permanent records of wind-vane position and smoke-release movement have been made in the form of color motion pictures and still photographs.

4.3.2 1:650 Scale Model

Figures 4.10 to 4.17 show typical examples of the effect of variations in wind speed, stack height and exit velocity on plume geometry and behavior. Figures 4.18 and 4.19 show typical cases in which the plume behavior is strongly influenced by stack downwash. Only a sample of photographs has been presented herein in order to expedite the process of report preparation. However, for each case tested, color motion pictures, color videotape and still photographs have been made and retained on file. Table 4.1 gives a listing of the motion pictures recorded.

4.4 Results of Concentration Measurements

By virtue of the constancy, from model to prototype, of the concentration coefficient, $\frac{\chi V_a D^2}{Q_s}$, the measured model concentrations of stack effluent were converted to prototype dimensions (ppm). The concentrations resulting from the operation of each individual stack (or group of stacks, in the instance of units 1-4) and several combinations of stacks (1-4 and 5; 1c and 5; 1c, 5 and 6; 1c, 5, 6and 7; 1c, 5, 6, 7 and 8) have been tabulated in Appendix A (Volume II of this report). Appendix B (Volume III of this report) contains figures presenting isopleths of concentration for the cases with individual stacks operating.

In the interpretation of the concentration data, it should be noted that the model air samples were withdrawn over a period corresponding to approximately one hour, prototype, in the absence of the large-scale eddies which can cause plume meandering in the prototype during the same time duration. Thus, the modeled concentrations represent an approximate upper limit which would be approached in the prototype if no plume meandering were to occur. According to the findings of Hino (1968), plume meandering could reduce the instantaneous concentrations to as little as 25 percent of the predicted values.

REFERENCES

Cermak, J. E. and J. Peterka, "Simulation of Wind Fields over Point Arguello, California, by Wind-Tunnel Flow over a Topographical Model," Final Report, U.S. Navy Contract N126(61756)34361 A (PMR), Colorado State University, CER65JEC-JAP64, December, 1966.

Cermak, J. E., "Laboratory Simulation of the Atmospheric Boundary Layer," AIAA Jl., Vol. 9, No. 9, pp. 1746-1754, September, 1971.

Halitsky, J., "Gas Diffusion near Buildings," Geophysical Sciences Laboratory Report No. 63-3, New York University, February, 1963.

Hino, M., "Maximum Ground-Level Concentration and Sampling Time," Atmospheric Environment, Vol. 2, pp. 149-165, 1968.

Lord, G. R. and H. J. Leutheusser, "Wind-Tunnel Modelling of Stack-Gas Discharge," Man and His Environment, Vol. 1 (M. A. Ward, Ed.) Pergamon Press, 1970.

Martin, J. E., "The Correlation of Wind Tunnel and Field Measurements of Gas Diffusion Using Kr-85 as a Tracer," Ph.D. Thesis, MMPP 272, University of Michigan, June, 1965.

FIGURES

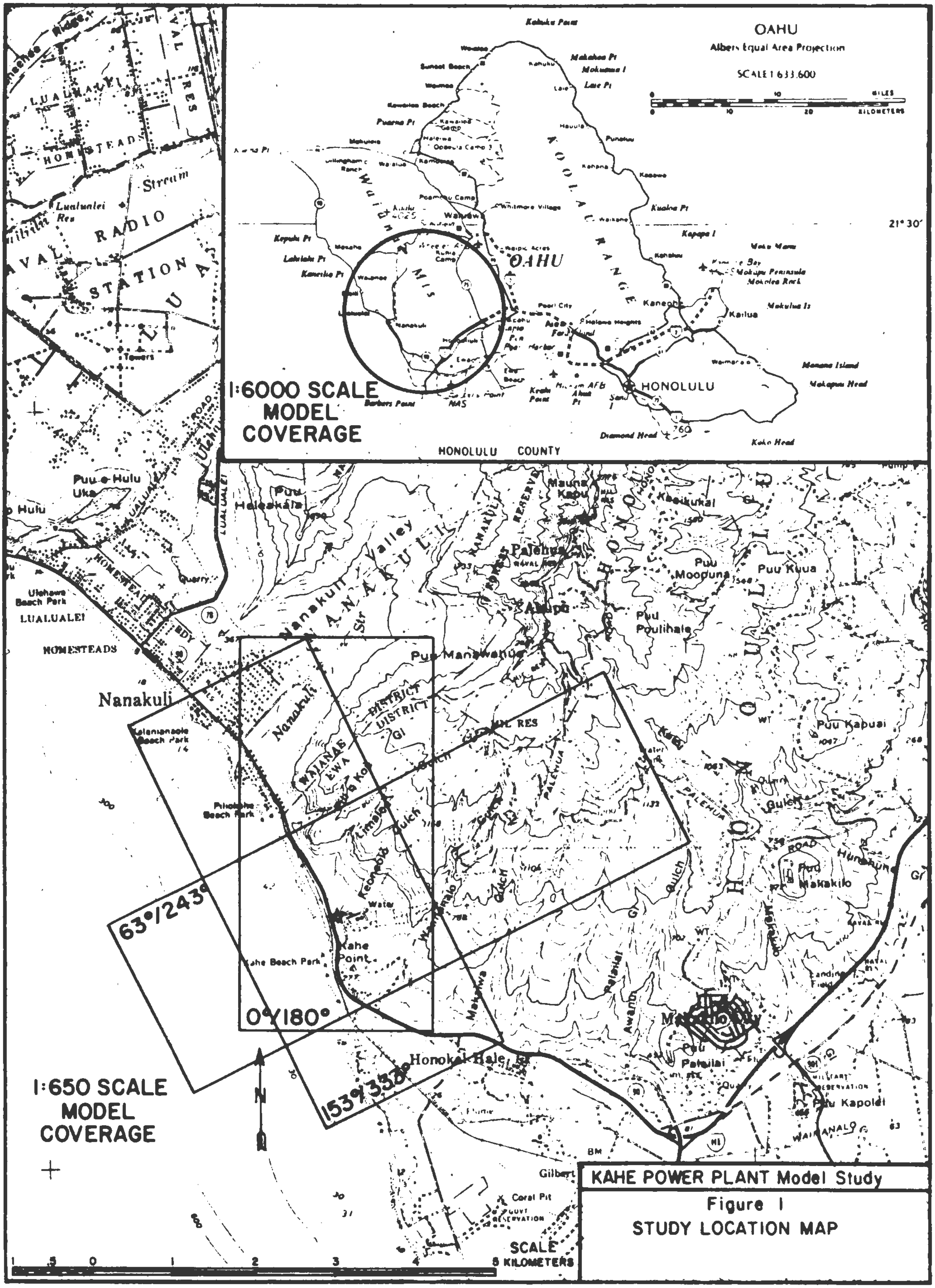

KAHE POWER PLANT Model Study

Figure 1

STUDY LOCATION MAP

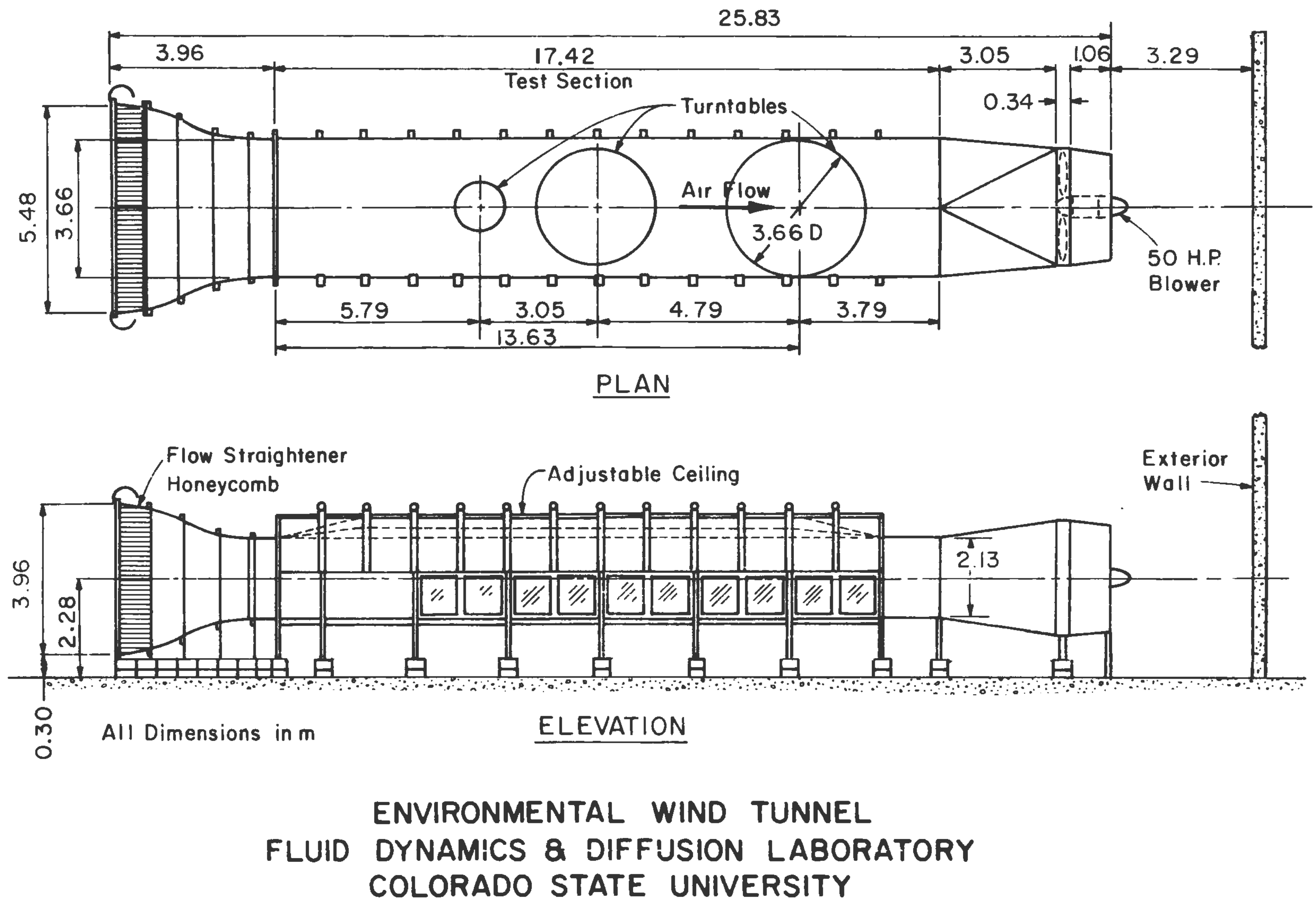

25.83
3.96
17.42
Test Section
3.05
1.06
3.29
0.34
Turntables
5.48
3.66
Air Flow
3.66 D
50 H.P. Blower
5.79
3.05
4.79
3.79
13.63
PLAN
Flow Straightener Honeycomb
Adjustable Ceiling
Exterior Wall
2.13
3.96
2.28
0.30
All Dimensions in m
ELEVATION
ENVIRONMENTAL WIND TUNNEL
FLUID DYNAMICS & DIFFUSION LABORATORY
COLORADO STATE UNIVERSITY

Figure 3.1

Figure 3.2. 1:6000 Scale Model in Wind Tunnel

Figure 3.3. 1:6000 Scale Model in Wind Tunnel, Velocity-Measuring Instruments in Foreground

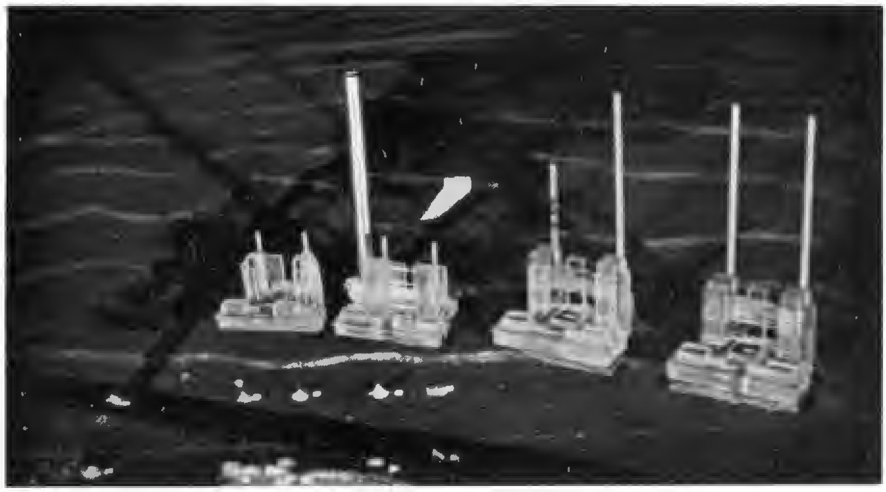

Figure 3.4. Model KEGP Plant Site (1:650 Scale, 137 m Stacks Shown)

Figure 3.5. Close-up of Kahe Bowl Area (1:6000 Scale Model) Showing Wind Vanes

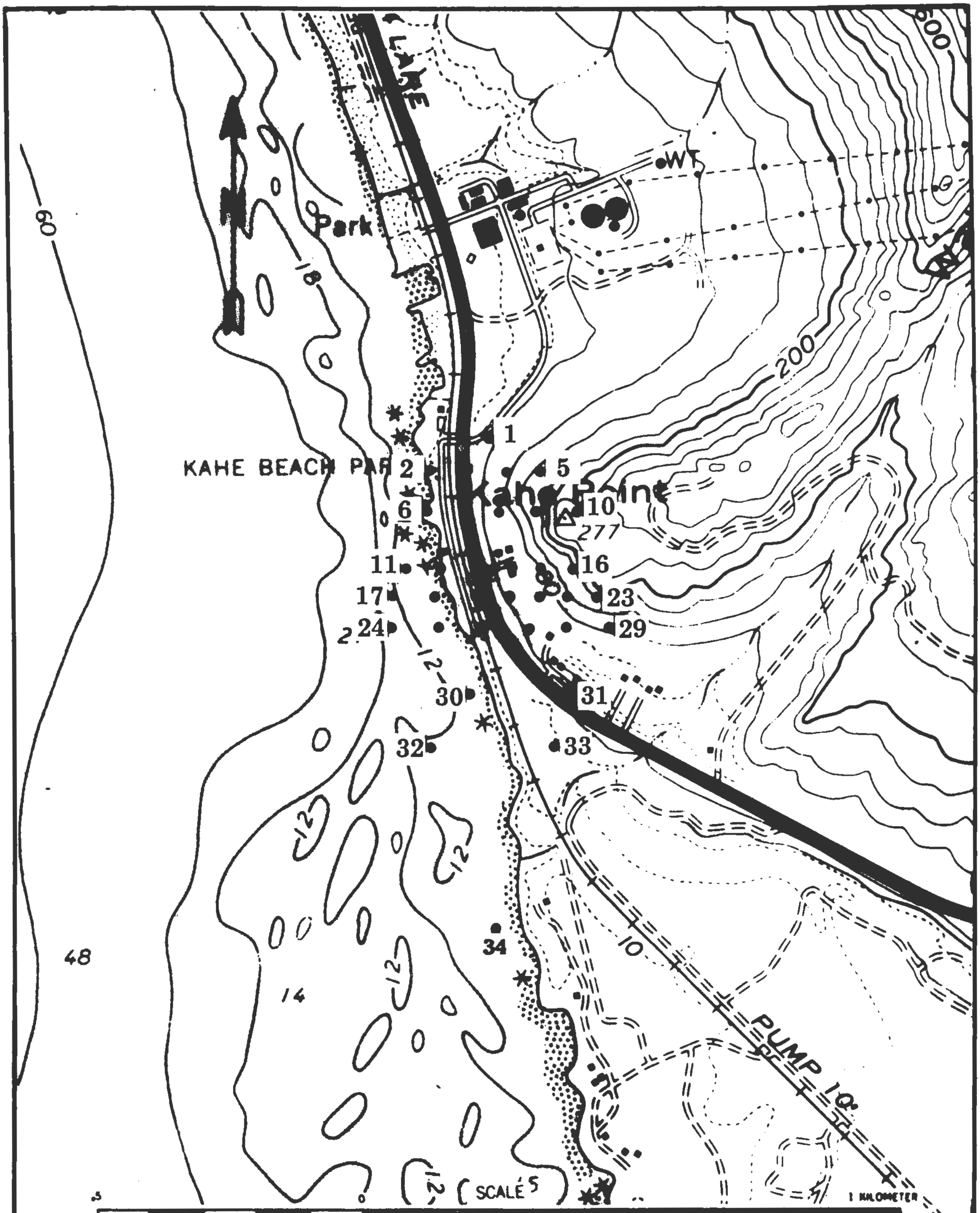

NOTE: EPA STN.1 = GRID POINT 1

KAHE POWER PLANT Model Study

Figure 3.6.1
SAMPLE GRID LOCATIONS
0° WIND DIRECTION

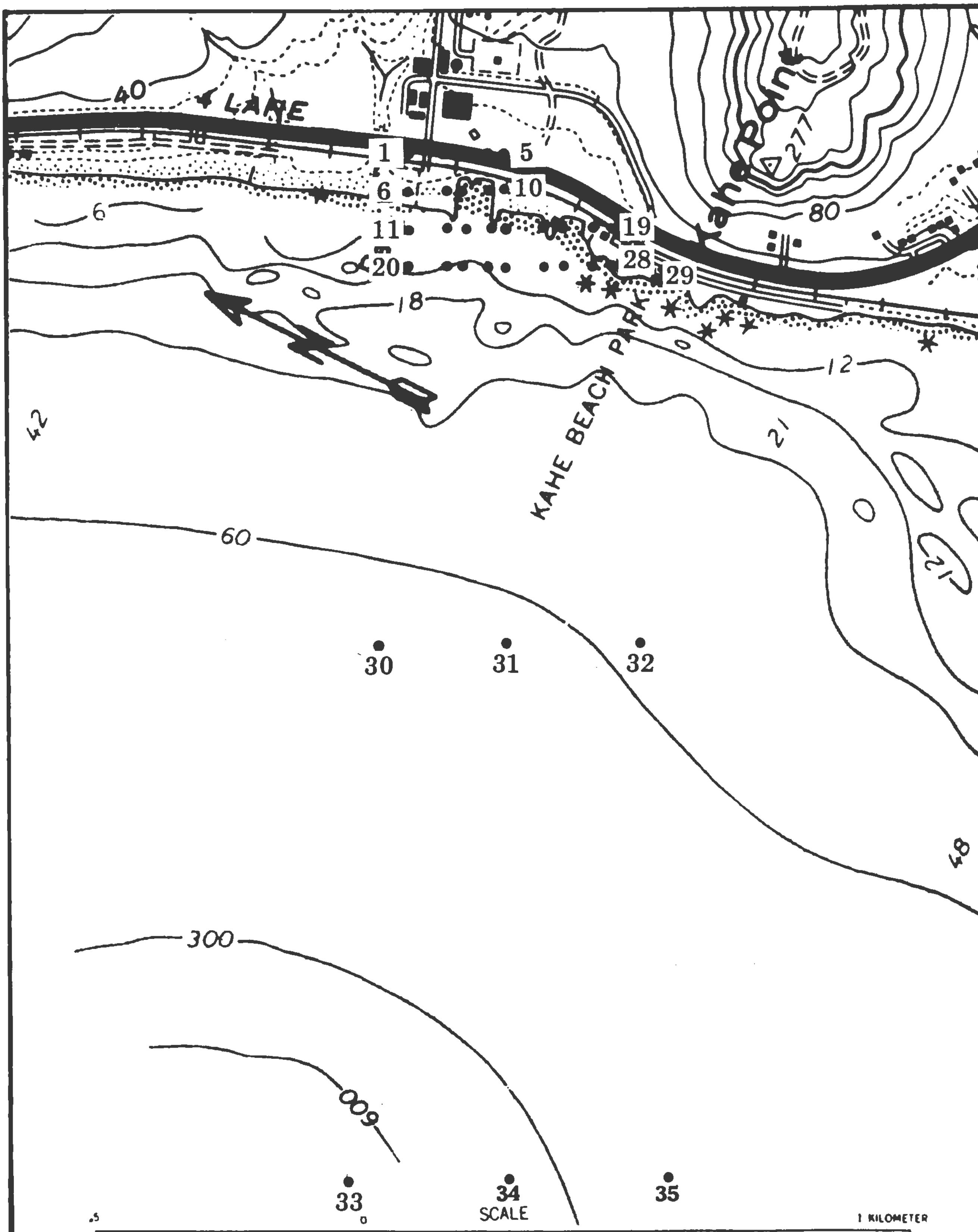

NOTE: EPA STN.2 = GRID POINT 4

KAHE POWER PLANT Model Study

Figure 3.6.2
SAMPLE GRID LOCATIONS
63° WIND DIRECTION

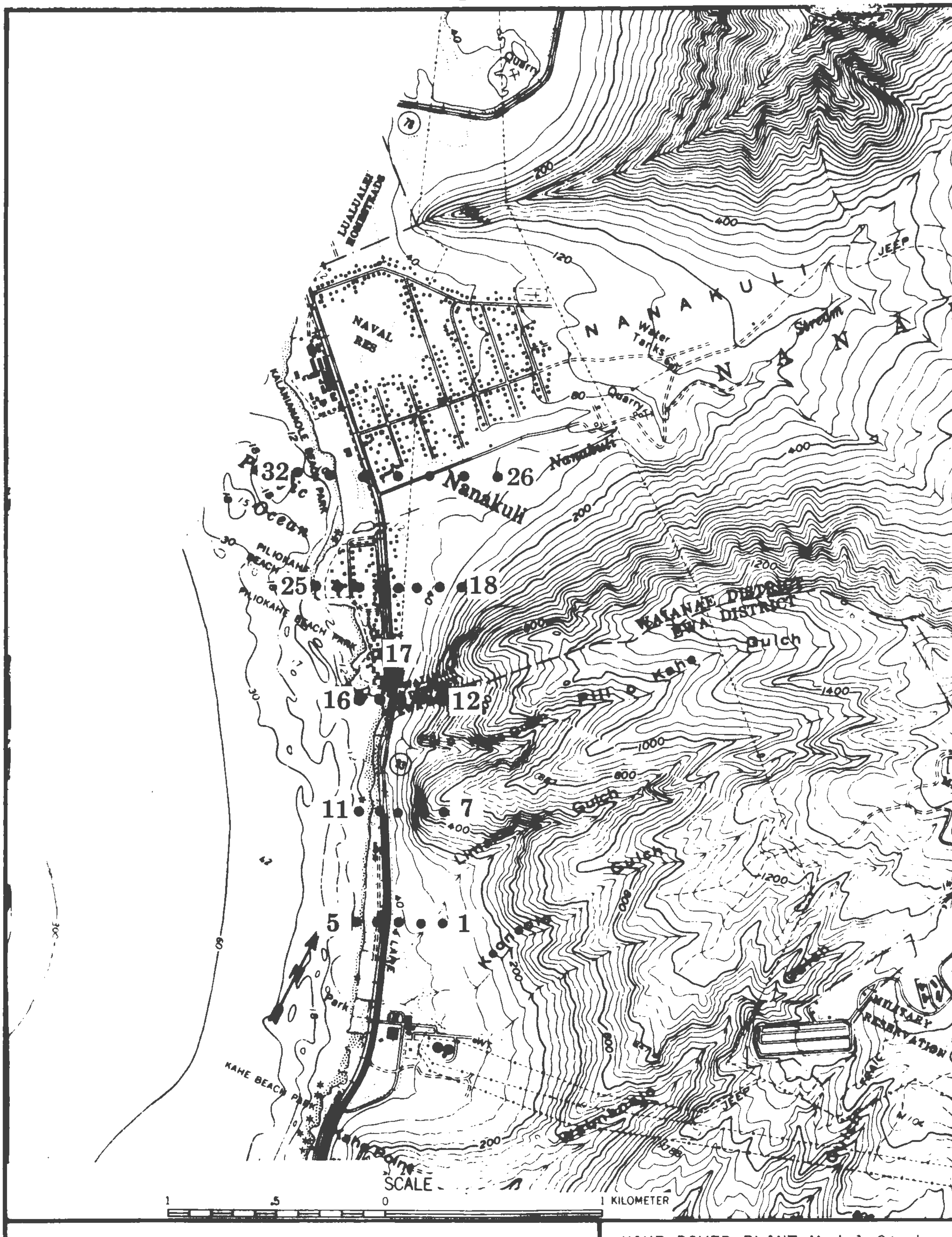

NOTE: EPA STN.3 = GRID POINT 17

KAHE POWER PLANT Model Study

Figure 3.6.3
SAMPLE GRID LOCATIONS
153° WIND DIRECTION

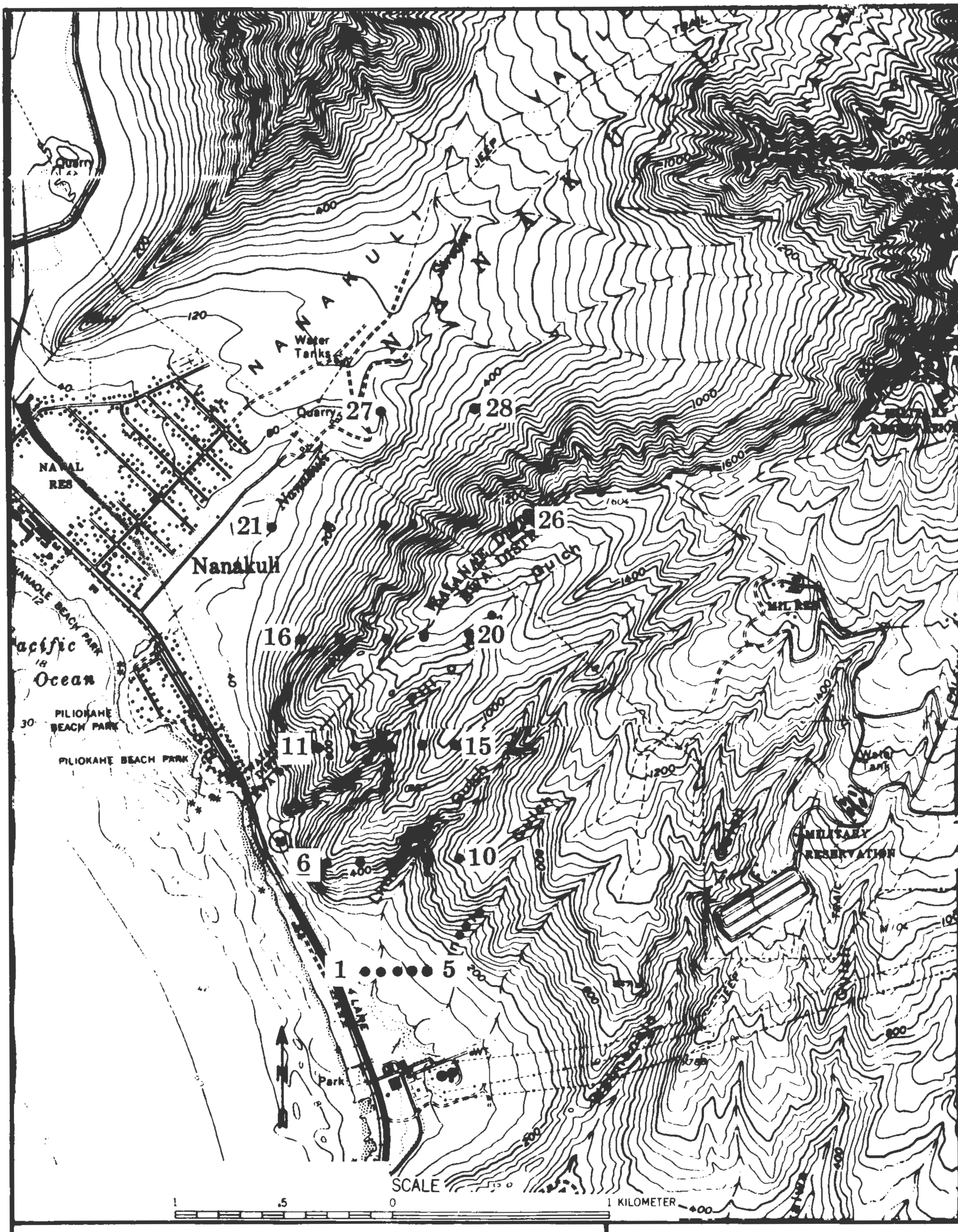

KAHE POWER PLANT Model Study
Figure 3.6.4 SAMPLE GRID LOCATIONS 180° WIND DIRECTION

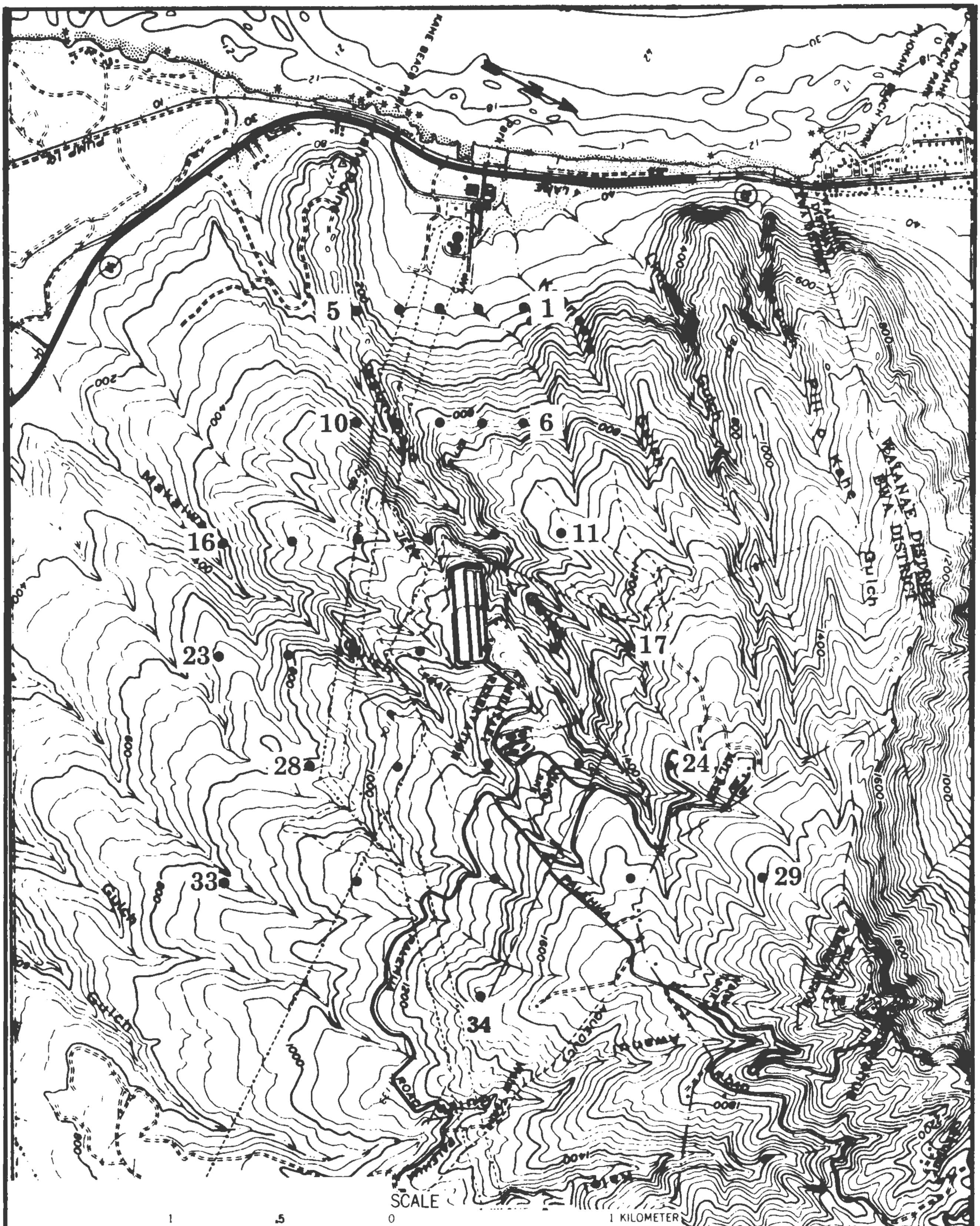

KAHE POWER PLANT Model Study

Figure 3.6.5
SAMPLE GRID LOCATIONS
243° WIND DIRECTION

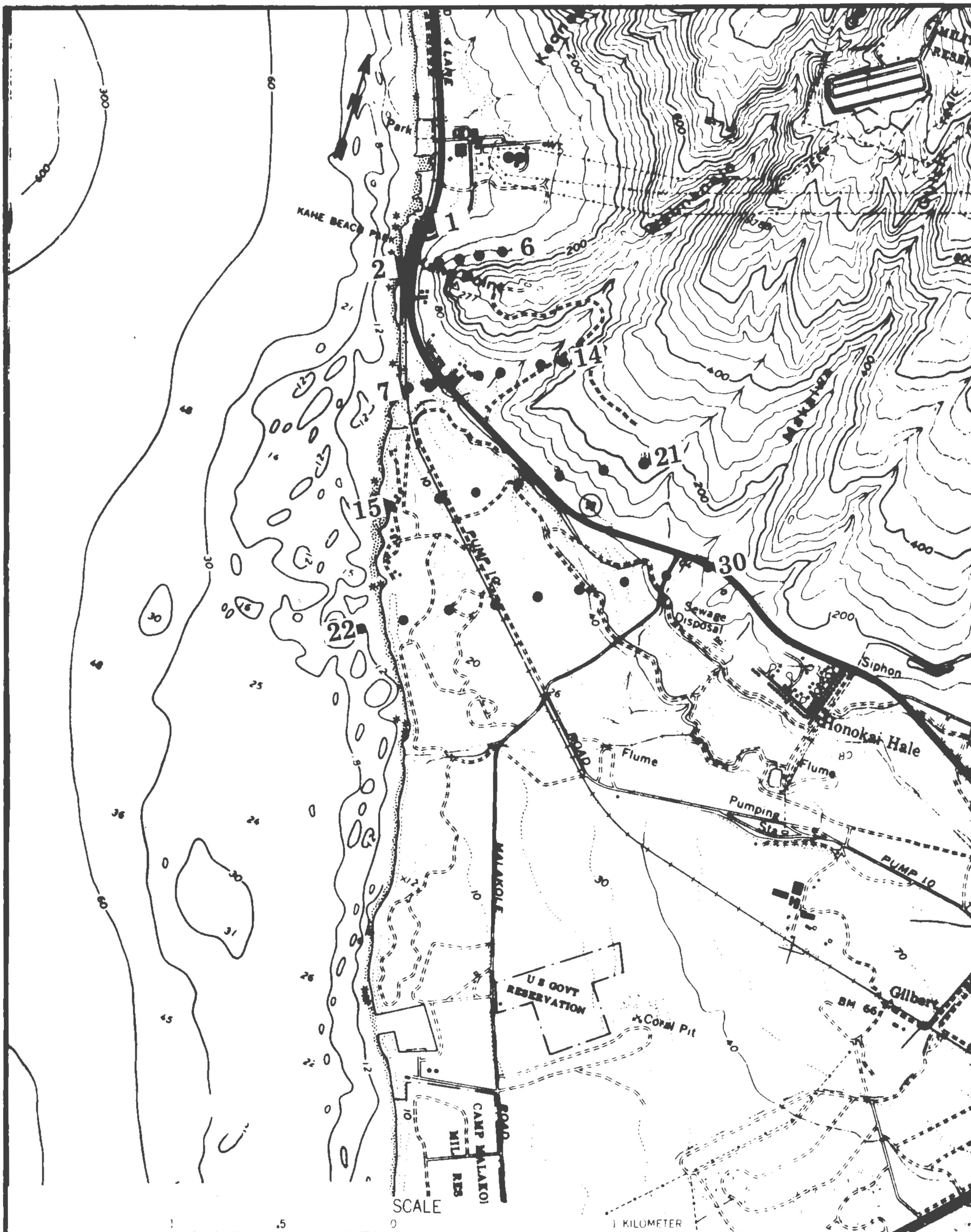

NOTE: EPA STN.1 = GRID POINT 1

KAHE POWER PLANT Model Study

Figure 3.6.6
SAMPLE GRID LOCATIONS
333° WIND DIRECTION

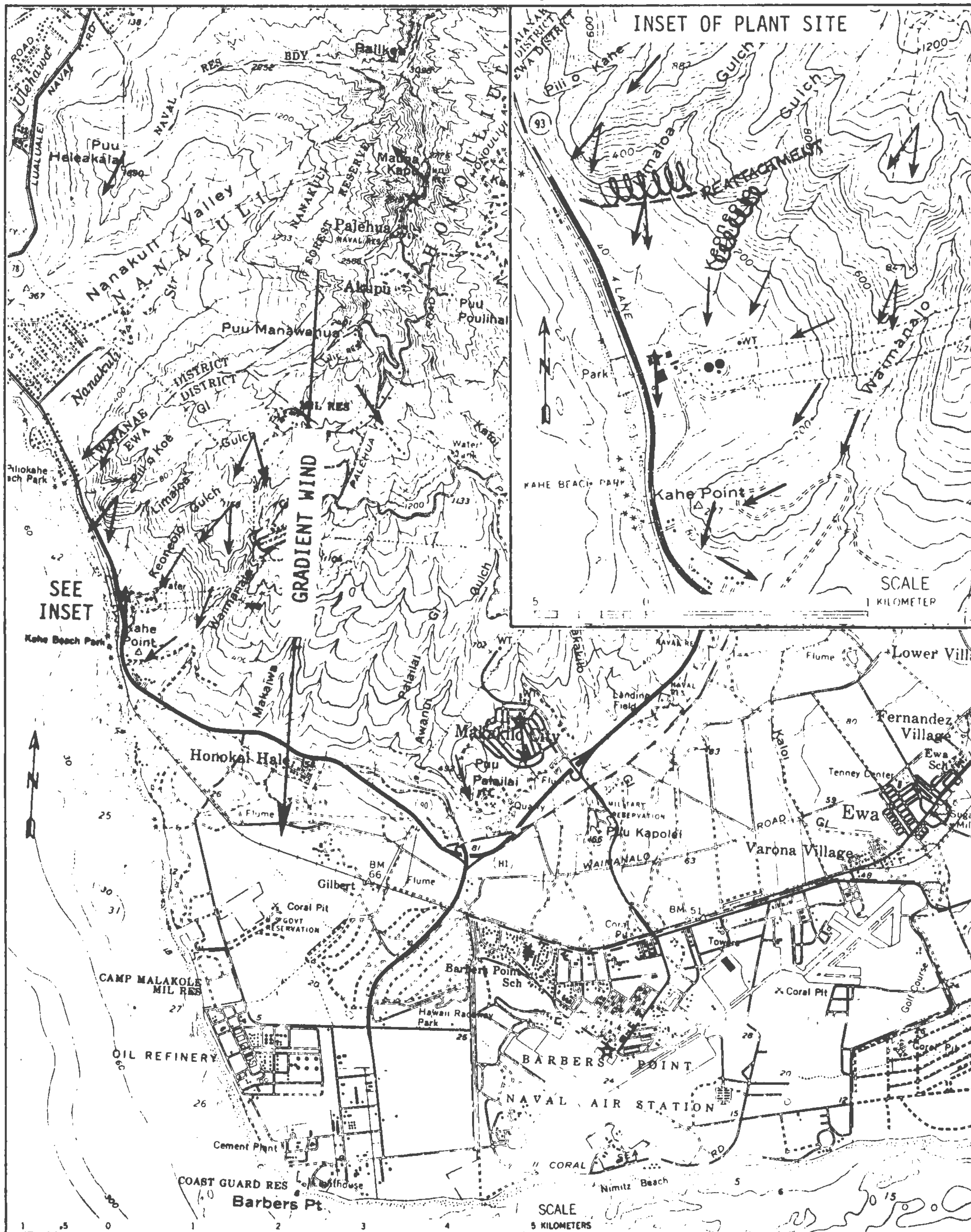

LEGEND:		KAHE POWER PLANT Model Study
Surface Wind Direction:	Steady → Fluctuating ⇇	Figure 4.1 Surface Wind Direction With Gradient Wind At 0°
Meteorological Station Site:	☆	

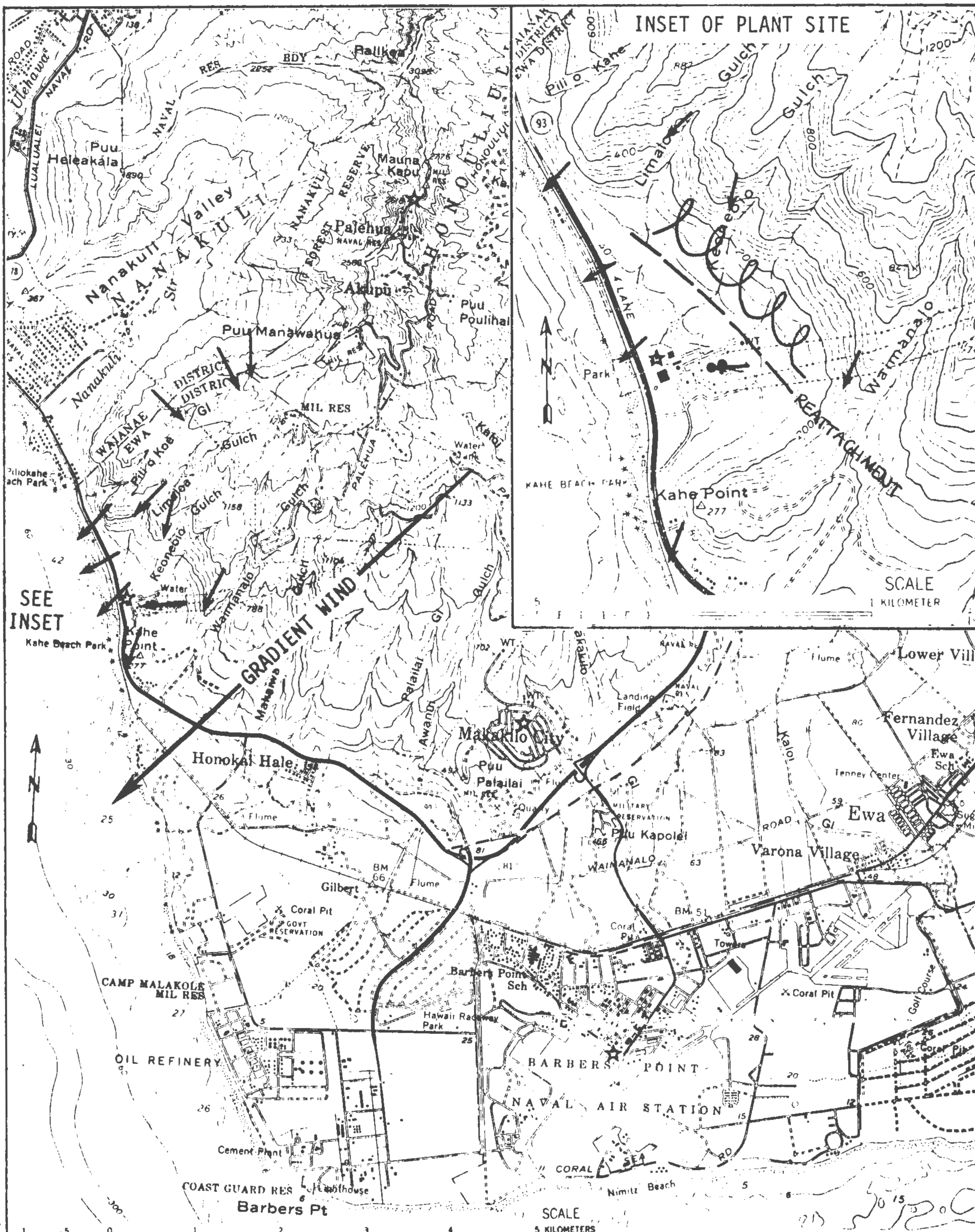

LEGEND:

Surface Wind Direction: Steady →
Fluctuating

Meteorological Station Site: ☆

KAHE POWER PLANT Model Study

Figure 4.2
Surface Wind Direction With Gradient Wind At 45°

LEGEND:

Surface Wind Direction: Steady →

Fluctuating ⇄

Meteorological Station Site: ☆

KAHE POWER PLANT Model Study

Figure 4.3
Surface Wind Direction With Gradient Wind At 62°

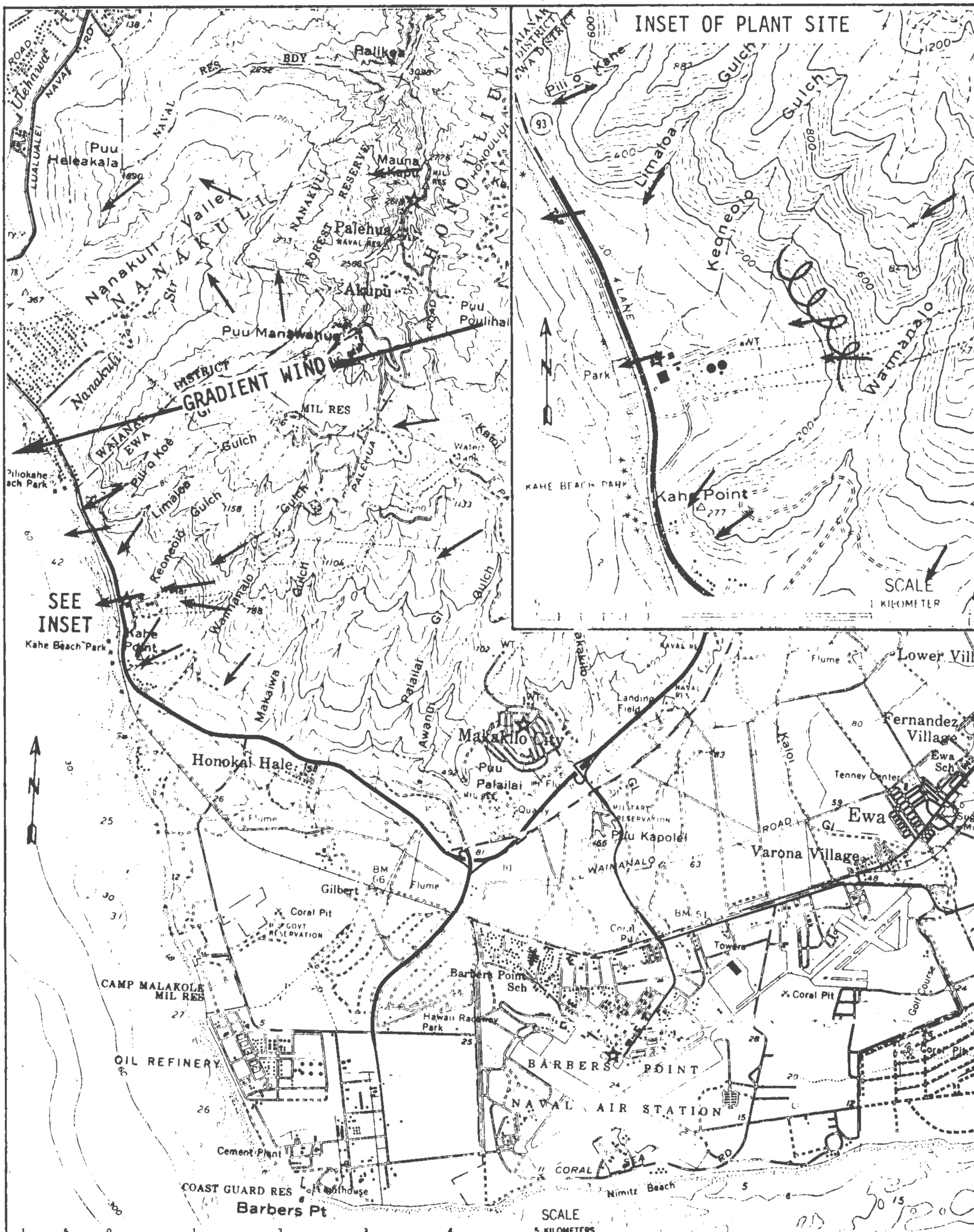

LEGEND:

Surface Wind Direction: Steady →, Fluctuating ⇄

Meteorological Station Site: ☆

KAHE POWER PLANT Model Study

Figure 4.4
Surface Wind Direction With Gradient Wind At 72°

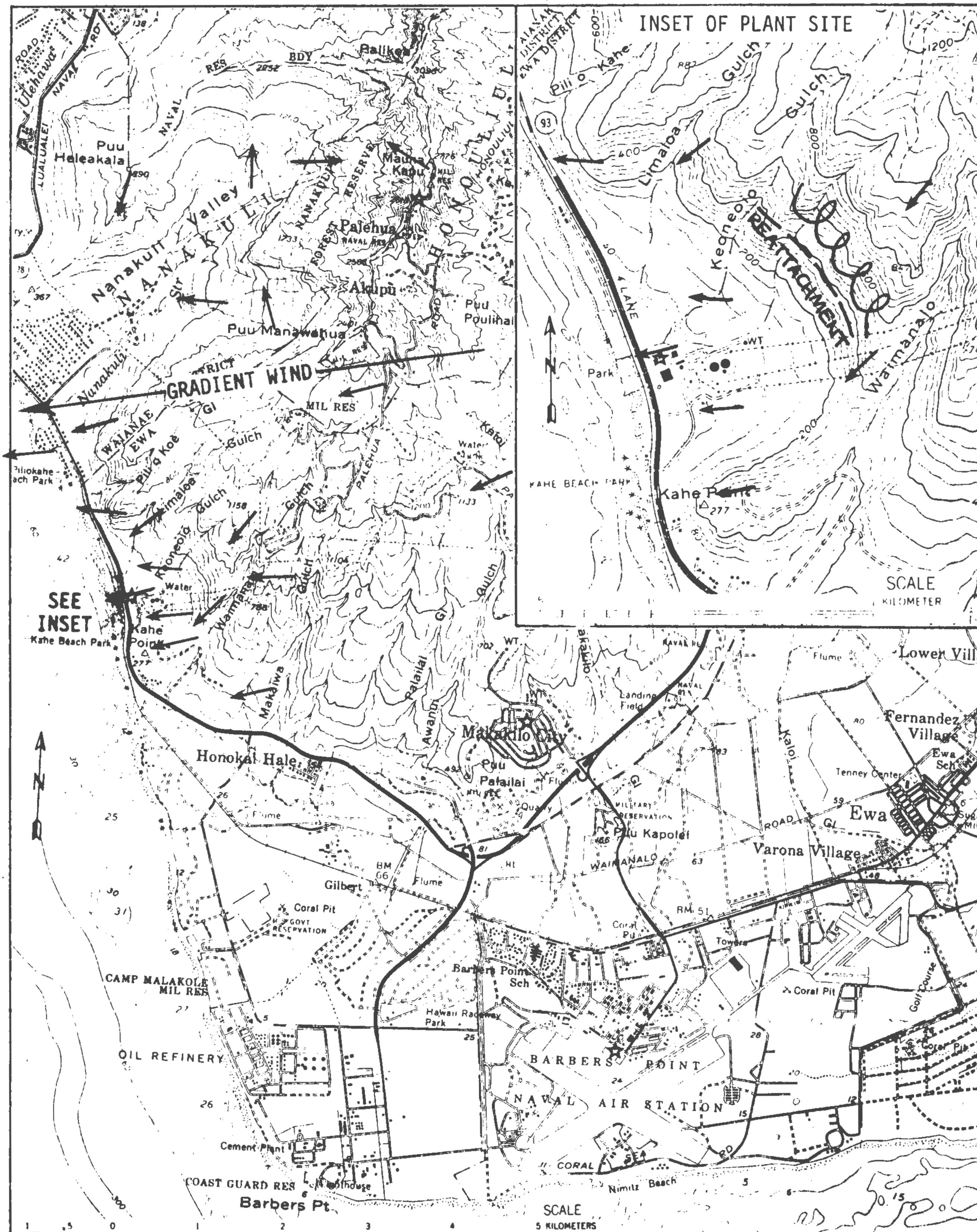

LEGEND:

Surface Wind Direction: Steady ⟶ Fluctuating

Meteorological Station Site: ☆

KAHE POWER PLANT Model Study

Figure 4.5
Surface Wind Direction With Gradient Wind At 79°

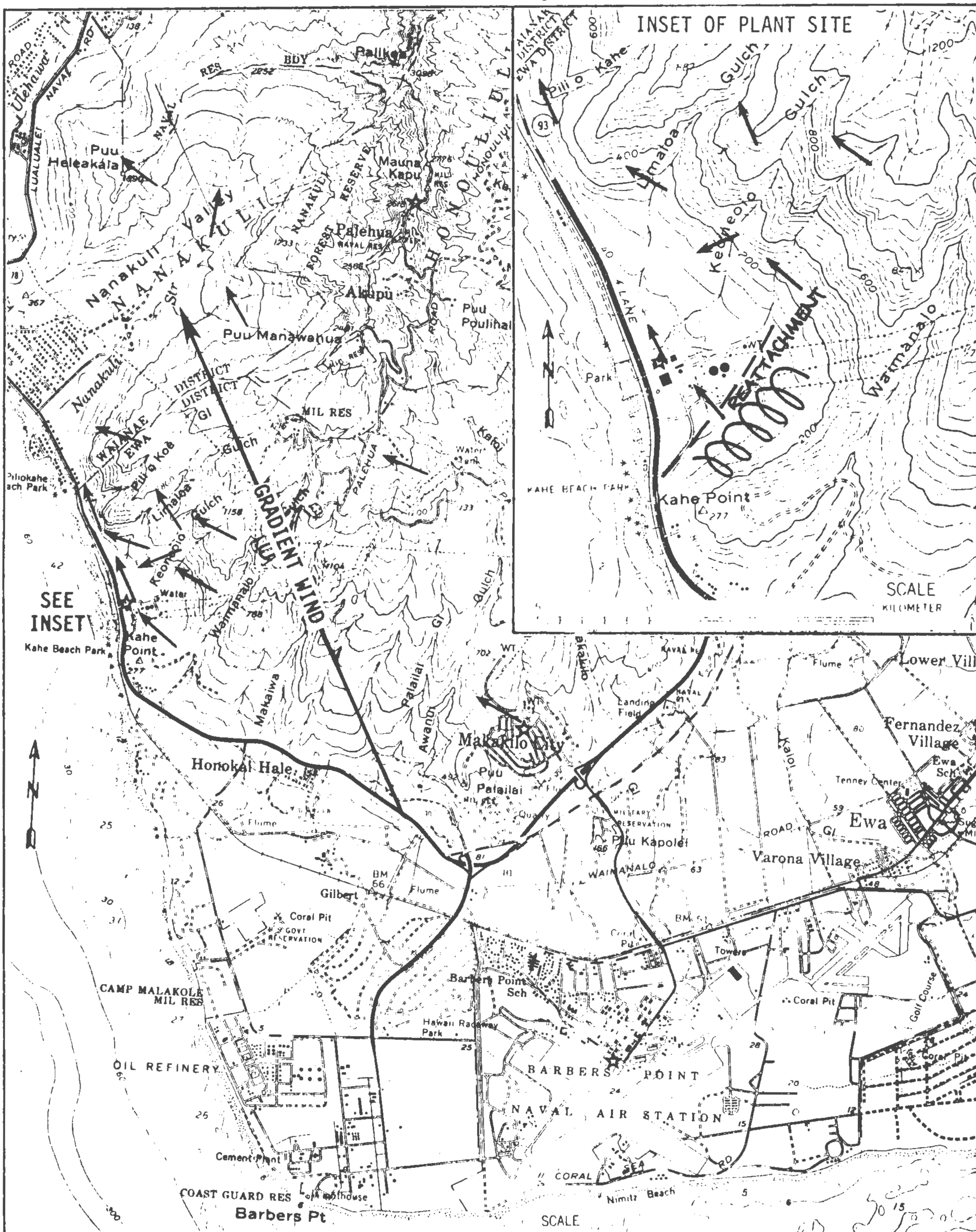

LEGEND:

Surface Wind Direction: Steady / Fluctuating

Meteorological Station Site: ☆

KAHE POWER PLANT Model Study

Figure 4.6
Surface Wind Direction With Gradient Wind At 153°

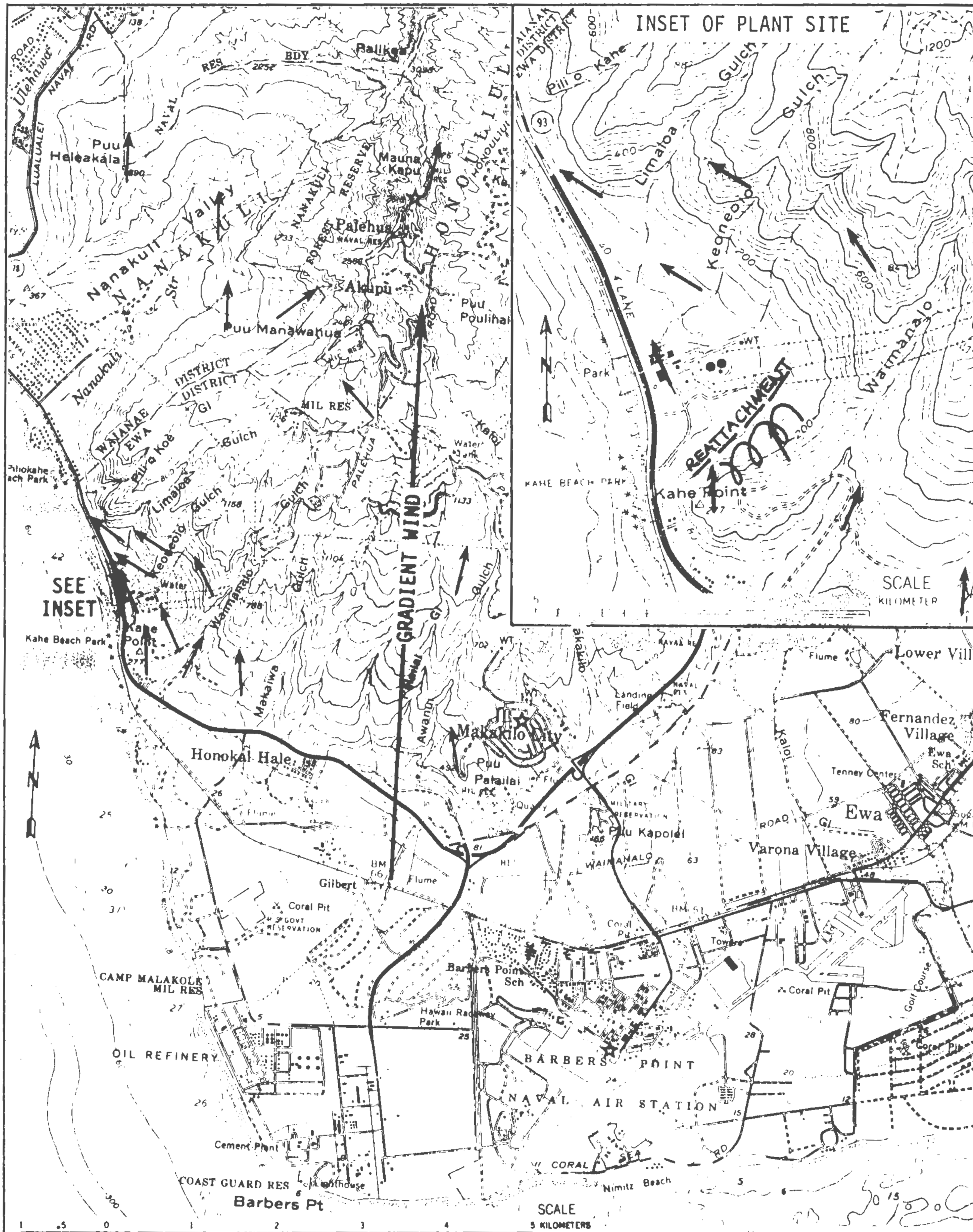

LEGEND:

Surface Wind Direction: Steady → Fluctuating

Meteorological Station Site: ☆

KAHE POWER PLANT Model Study

Figure 4.7
Surface Wind Direction With Gradient Wind At 180°

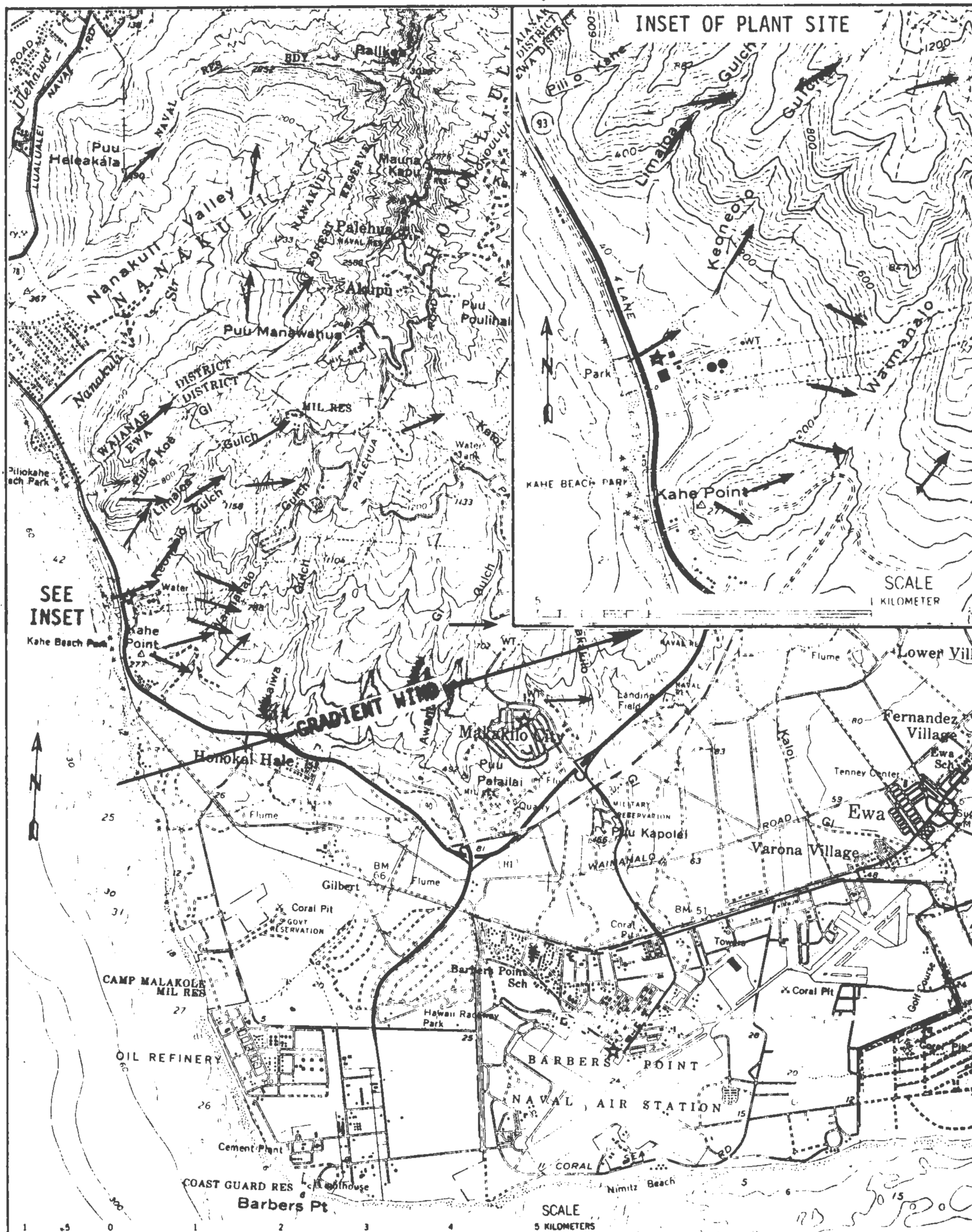

LEGEND:	KAHE POWER PLANT Model Study
Surface Wind Direction: Steady ⟶ Fluctuating ⇄ Meteorological Station Site: ☆	Figure 4.8 Surface Wind Direction With Gradient Wind At 252°

LEGEND:	KAHE POWER PLANT Model Study
Surface Wind Direction: Steady ⟶ Fluctuating	Figure 4.9 Surface Wind Direction With Gradient Wind At 333°
Meteorological Station Site: ☆	

Figure 4.10 Stack 1C: wind 6.7 m/s at 333° stack height 91 m, 100% operating level

Figure 4.11 Stack 1C: wind 13.4 m/s at 333°, stack height 91 m, 100% operating level

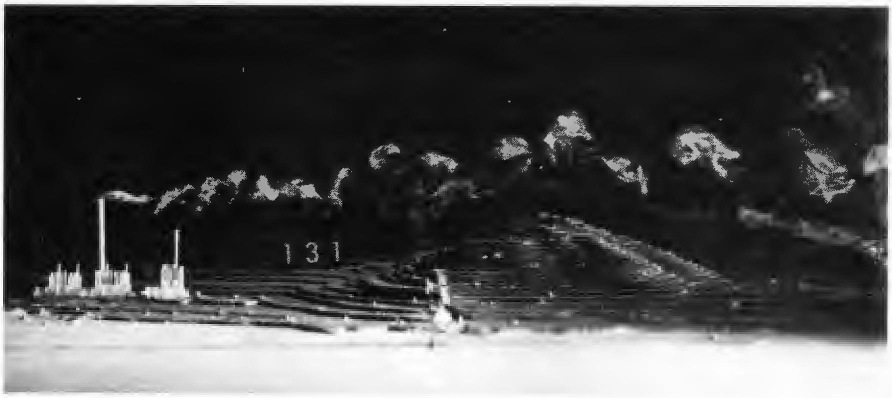

Figure 4.12 Stack 1c: wind 6.7 m/s at 333°, stack height 137 m, 100% operating level

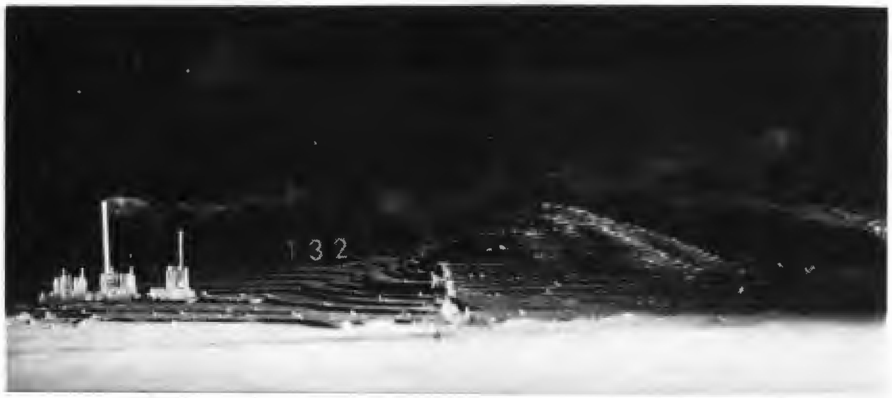

Figure 4.13 Stack 1c: wind 13.4 m/s at 333°, stack height 183 m, 100% operating level

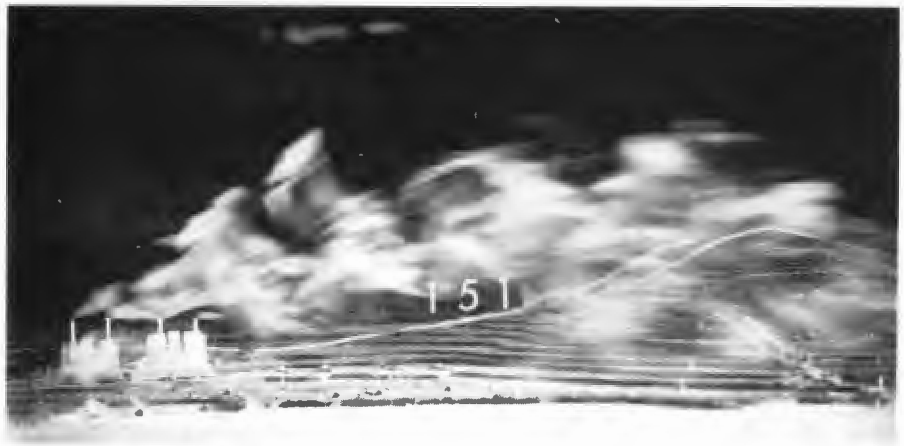

Figure 4.14 Stacks 1-4: wind 6.7 m/s at 0°,
100% operating level

Figure 4.15 Stacks 1-4: wind 13.4 m/s at 0°,
100% operating level

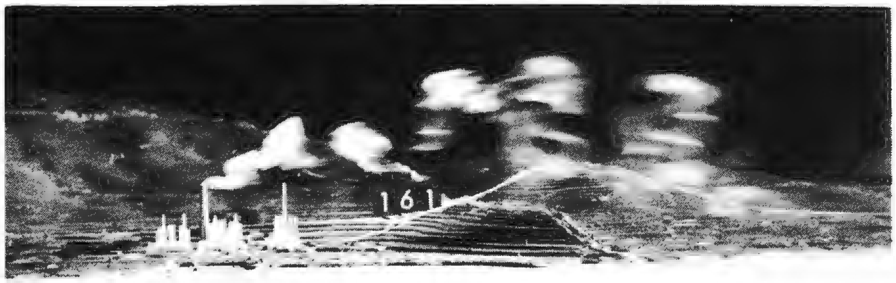

Figure 4.16 Stack 1c: wind 6.7 m/s at 0°, stack height 91 m, 75% operating level

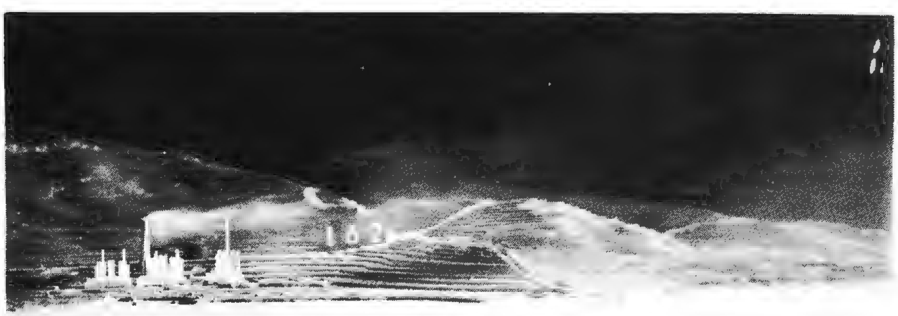

Figure 4.17 Stack 1c: wind 13.4 m/s at 0°, stack height 91 m, 75% operating level

Figure 4.18 Downwash on stack 1c: wind 6.7 m/s at 63°, stack height 183 m, 75% operating level

Figure 4.19 Downwash on stack 6: wind 13.4 m/s at 63°, stack height 183 m, 100% operating level

Table 2.1.1. KEGP Model Parameters (1:650 Scale)

Parameter	Unit					
	1	2	3	4	5, 6, 7, 8	1C
Stack Velocity (m/s)						
100% Load	0.62	0.60	0.49	0.54	0.40	0.20
75% Load	0.47	0.45	0.37	0.41	0.30	0.15
I.D. of Stack (m)	0.0048	0.0048	0.0048	0.0048	0.0072	0.016
Stack Discharge ($m^3/s \times 10^5$)						
100% Load	1.11	1.08	0.88	0.97	1.61	4.04
75% Load	0.86	0.83	0.71	0.78	1.36	3.03
$F_r = \frac{V_s^2}{\gamma D}$						
100% Load	29.1	27.2	18.4	22.1	7.84	0.90
75% Load	16.4	15.4	10.4	12.5	4.41	0.50
$R = \frac{V_s}{V_a}$ (V_a = 0.26, 0.52 m/s)						
100% Load	2.37, 1.19	2.29, 1.14	1.89, 0.95	2.08, 1.04	1.54, 0.77	0.77, 0.38
75% Load	1.78, 0.89	1.72, 0.86	1.42, 0.71	1.56, 0.78	1.16, 0.58	0.58, 0.29
Source Strength (ppm $\times 10^{-4}$)	5.0	5.0	5.0	5.0	7.3, 13.8, 3.8, 7.3	5.0
Effluent Temp. (°K)	293.	(ALL)				
Effluent Density, ρ_s (kg/m^3)	0.73	(ALL)				
Ambient Temp. (°K)	293.					
Ambient Pressure (mb)	850.					
Ambient Density, ρ_a (kg/m^3)	1.02					
$\gamma = \frac{\rho_a - \rho_s}{\rho_a}$	0.28	(ALL)				

Table 2.1.2. KEGP Prototype Parameters

Parameter	Unit					
	1	2	3	4	5, 6, 7, 8	1C
Stack Velocity (m/s)						
100% Load	15.91	15.34	12.71	13.93	10.30	5.12
75% Load	11.93	11.51	9.53	10.45	7.73	3.84
I.D. of Stack (m)	3.15	3.15	3.20	3.20	4.93	10.67
Stack Discharge (m^3/s)						
100% Load	124.0	119.5	102.0	112.0	196.5	458.0
75% Load	93.0	90.0	76.5	84.0	147.5	343.5
$F_r = \frac{V_s^2}{\gamma D}$						
100% Load	29.1	27.2	18.4	22.1	7.84	0.90
75% Load	16.4	15.4	10.4	12.5	4.41	0.50
$R = \frac{V_s}{V_a}$ (V_a = 6.71, 13.4 m/s)						
100% Load	2.37, 1.19	2.29, 1.14	1.89, 0.95	2.08, 1.04	1.54, 0.77	0.77, 0.38
75% Load	1.78, 0.89	1.72, 0.86	1.42, 0.71	1.56, 0.78	1.16, 0.58	0.58, 0.29
Source Strength (ppm)	863.	834.	834.	839.	840.	840.
Effluent Temp. (°K)	404.	404.	406.	406.	407.	405.
Effluent Density, ρ_s (kg/m^3)	0.87	(ALL)				
Ambient Temp. (°K)	293.					
Ambient Density, ρ_a (kg/m^3)	1.20					
Ambient Pressure (mb)	1000.					
$\gamma = \frac{\rho_a - \rho_s}{\rho_a}$	0.28	(ALL)				

Table 4.1. 1:650 Model Test Program--Motion-Picture Sequence of Flow Visualizations

Run	Wind Direction (deg. az.)	Units Present	Units Operating	Stack Heights (m)	Operating Level (%)	Wind Velocity (m/s)
1	63	1	1	45.	100	6.7
2	"	"	"	"	"	13.4
3	"	"	"	"	75	6.7
4	"	"	"	"	"	13.4
5	"	1,2	1,2	45.	100	6.7
6	"	"	"	"	"	13.4
7	"	"	"	"	75	6.7
8	"	"	"	"	"	13.4
9	"	1,2,3	1,2,3	45.	100	6.7
10	"	"	"	"	"	13.4
11	"	"	"	"	75	6.7
12	"	"	"	"	"	13.4
13	"	1,2,3,4	1,2,3,4	45.	100	6.7
14	"	"	"	"	"	13.4
15	"	"	"	"	75	6.7
16	"	"	"	"	"	13.4
17	"	1,2,3,4,5	5	91.5	100	6.7
18	"	"	"	"	"	13.4
19	"	"	"	"	75	6.7
20	"	"	"	"	"	13.4
21	"	1,2,3,4,5, 1C	1C	91.5	100	6.7
22	"	"	"	"	"	13.4
23	"	"	"	"	75	6.7
24	"	"	"	"	"	13.4
25	"	"	"	137.	100	6.7
26	"	"	"	"	"	13.4
27	"	"	"	"	75	6.7
28	"	"	"	"	"	13.4
29	"	1C,1,2,3,4, 5,6	6	91.5	100	6.7
30	"	"	"	"	"	13.4
31	"	"	"	137.	100	6.7
32	"	"	"	"	"	13.4
33	"	"	"	183.	100	6.7
34	"	"	"	"	"	13.4
35	153	1,2,3,4	1,2,3,4	45.	100	6.7
36	"	"	"	"	"	13.4
37	"	"	"	"	75	6.7
38	"	"	"	"	"	13.4
39	"	1,2,3,4,5	5	91.5	100	6.7
40	"	"	"	"	"	13.4
41	"	"	"	"	75	6.7
42	"	"	"	"	"	13.4
43	"	1C,1,2,3,4, 5	1C	91.5	100	6.7
44	"	"	"	"	"	13.4

Table 4.1 (continued). 1:650 Model Test Program--Motion-Picture Sequence of Flow Visualizations

Run	Wind Direction (deg. az.)	Units Present	Units Operating	Stack Heights (m)	Operating Level (%)	Wind Velocity (m/s)
45	153	1C,1,2,3,4,5	1C	91.5	75	6.7
46	"	"	"	"	"	13.4
47	"	"	"	137.	100	6.7
48	"	"	"	"	"	13.4
49	"	"	"	"	75	6.7
50	"	"	"	"	"	13.4
51	"	1C,1,2,3,4, 5,6	6	91.5	100	6.7
52	"	"	"	"	"	13.4
53	"	"	"	137.	100	6.7
54	"	"	"	"	"	13.4
55	"	"	"	183.	100	6.7
56	"	"	"	"	"	13.4
57	"	1C,1,2,3,4, 5,6,7	7	91.5	100	6.7
58	"	"	"	"	"	13.4
59	"	"	"	137.	100	6.7
60	"	"	"	"	"	13.4
61	"	"	"	183.	100	6.7
62	"	"	"	"	"	13.4
63	"	1C,1,2,3,4, 5,6,7,8	8	183.	100	6.7
64	"	"	"	"	"	13.4
65	"	1C,1,2,3,4, 5,6,7,8	1C,5,6,7,8	137.	100	6.7
66	"	"	"	"	"	13.4
67	180	1,2,3,4	1,2,3,4	45.	100	6.7
68	"	"	"	"	"	13.4
69	"	"	"	"	75	6.7
70	"	"	"	"	"	13.4
71	"	5,1,2,3,4	5	91.5	100	6.7
72	"	"	"	"	"	13.4
73	"	"	"	"	75	6.7
74	"	"	"	"	"	13.4
75	"	1C,1,2,3,4, 5	1C	91.5	100	6.7
76	"	"	"	"	"	13.4
77	"	"	"	"	75	6.7
78	"	"	"	"	"	13.4
79	"	"	"	137.	100	6.7
80	"	"	"	"	"	13.4
81	"	"	"	"	75	6.7
82	"	"	"	"	"	13.4
83	"	1C,1,2,3,4, 5,6	6	91.5	100	6.7
84	"	"	"	"	"	13.4
85	"	"	"	137.	100	6.7

Table 4.1 (continued). 1:650 Model Test Program--Motion-Picture Sequence of Flow Visualizations

Run	Wind Direction (deg. az.)	Units Present	Units Operating	Stack Heights (m)	Operating Level (%)	Wind Velocity (m/s)
86	180	1C,1,2,3,4,5,6	6	137	100	13.4
87	"	"	"	183.	100	6.7
88	"	"	"	"	"	13.4
89	243	1,2,3,4	1,2,3,4	45.	100	6.7
90	"	"	"	"	"	13.4
91	"	"	"	"	75	6.7
92	"	"	"	"	"	13.4
93	"	1,2,3,4,5	5	91.5	100	6.7
94	"	"	"	"	"	13.4
95	"	"	"	"	75	6.7
96	"	"	"	"	"	13.4
97	"	1,2,3,4,5, 1C	1C	91.5	100	6.7
98	"	"	"	"	"	13.4
99	"	"	"	"	75	6.7
100	"	"	"	"	"	13.4
101	"	"	"	137.	100	6.7
102	"	"	"	"	"	13.4
103	"	"	"	"	75	6.7
104	"	"	"	"	"	13.4
105	"	1,2,3,4,5, 1C,6	6	91.5	100	6.7
106	"	"	"	"	"	13.4
107	"	"	"	137.	100	6.7
108	"	"	"	"	"	13.4
109	"	"	"	183.	100	6.7
110	"	"	"	"	"	13.4
111		1,2,3,4,5, 1C,6,7	7	91.5	100	6.7
112	"	"	"	"	"	13.4
113	"	"	"	137.	100	6.7
114	"	"	"	"	"	13.4
115	"	"	"	183.	100	6.7
116	"	"	"	"	"	13.4
117	"	1,2,3,4,5, 1C,6,7,8	8	183.	100	6.7
118	"	"	"	"	"	13.4
119	333	1,2,3,4	1,2,3,4	45.	100	6.7
120	"	"	"	"	"	13.4
121	"	"	"	"	75	6.7
122	"	"	"	"	"	13.4
123	"	1,2,3,4,5	5	91.5	100	6.7
124	"	"	"	"	"	13.4
125	"	"	"	"	75	6.7
126	"	"	"	"	"	13.4
127	"	1,2,3,4,5, 1C	1C	91.5	100	6.7

Table 4.1 (continued). 1:650 Model Test Program--Motion-Picture Sequence of Flow Visualizations

Run	Wind Direction (deg. az.)	Units Present	Units Operating	Stack Heights (m)	Operating Level (%)	Wind Velocity (m/s)
128	333	1C,1,2,3, 4,5	1C	91.5	100	13.4
129	"	"	"	"	75	6.7
130	"	"	"	"	"	13.4
131	"	"	"	137.	100	6.7
132	"	"	"	"	"	13.4
133	"	"	"	"	75	6.7
134	"	"	"	"	"	13.4
135	"	1,2,3,4,5, 6,1C	6	91.5	100	6.7
136	"	"	"	"	"	13.4
137	"	"	"	137.	100	6.7
138	"	"	"	"	"	13.4
139	"	"	"	183.	100	6.7
140	"	"	"	"	"	13.4
141	"	1,2,3,4,5, 6,7,1C	7	91.5	100	6.7
142	"	"	"	"	"	13.4
143	"	"	"	137.	100	6.7
144	"	"	"	"	"	13.4
145	"	"	"	183.	100	6.7
146	"	"	"	"	"	13.4
147	"	1,2,3,4,5, 1C,6,7,8	8	137.	100	6.7
148	"	"	"	"	"	13.4
149	"	"	1C,5,6,7,8	137.	100	6.7
150	"	"	"	"	"	13.4
151	0	1,2,3,4	1,2,3,4	45.	100	6.7
152	"	"	"	"	"	13.4
153	"	"	"	"	75	6.7
154	"	"	"	"	"	13.4
155	"	1,2,3,4,5	5	91.5	100	6.7
156	"	"	"	"	"	13.4
157	"	"	"	"	75	6.7
158	"	"	"	"	"	13.4
159	"	1,2,3,4,5, 1C	1C	91.5	100	6.7
160	"	"	"	"	"	13.4
161	"	"	"	"	75	6.7
162	"	"	"	"	"	13.4
163	"	"	"	137.	100	6.7
164	"	"	"	"	"	13.4
165	"	"	"	"	75	6.7
166	"	"	"	"	"	13.4
167	"	1,2,3,4,5, 1C,6	6	91.5	100	6.7
168	"	"	"	"	"	13.4
169	"	"	"	137.	100	6.7

Table 4.1 (continued). 1:650 Model Test Program--Motion-Picture Sequence of Flow Visualizations

Run	Wind Direction (deg. az.)	Units Present	Units Operating	Stack Heights (m)	Operating Level (%)	Wind Velocity (m/s)
170	0	1C, 1,2,3, 4.5.6	6	137	100	13.4
171	"	"	"	183.	100	6.7
172	"	"	"	"	"	13.4

Table 4.2. 1:650 Model Test Program--Concentrations

Run	Wind Direction (deg. az.)	Units Present	Units Operating	Stack Heights (m)	Operating Level (%)	Wind Velocity (m/s)
1	63	1,2,3,4,5	1,2,3,4,5	45. (1,2,3,4) 91.5 (5)	100	6.7
2	"	"	"	"	"	13.4
3	"	"	"	"	75	6.7
4	"	"	"	"	"	13.4
5	"	1C, 1,2,3, 4,5,6,7,8	1C,6,7,8	91.5 (All)	100	6.7
6	"	"	"	"	"	13.4
7	"	"	"	"	75	6.7
8	"	"	"	"	"	13.4
9	"	"	"	137. (All)	100	6.7
10	"	"	"	"	"	13.4
11	"	"	"	"	75	6.7
12	"	"	"	"	"	13.4
13	"	"	"	183. (All)	100	6.7
14	"	"	"	"	"	
15	153	1,2,3,4,5	1,2,3,4,5	45. (1,2,3,4) 91.5 (5)	100	6.7
16	"	"	"	"	"	13.4
17	"	"	"	"	75	6.7
18	"	"	"	"	"	13.4
19	"	1C,1,2,3,4, 5,6,7,8	1C,6,7,8	91.5 (All)	100	6.7
20	"	"	"	"	"	13.4
21	"	"	"	"	75	6.7
22	"	"	"	"	"	13.4
23	"	"	"	137. (All)	100	6.7
24	"	"	"	"	"	13.4
25	"	"	"	183.	100	6.7
26	"	"	"	"	"	13.4
27	180	1,2,3,4,5	1,2,3,4,5	45. (1,2,3,4) 91.5 (5)	100	6.7
28	"	"	"	"	"	13.4
29	"	"	"	"	75	6.7
30	"	"	"	"	"	13.4
31	"	1C,1,2,3,4, 5,6,7,8	1C,6,7,8	91.5	100	6.7
32	"			"	"	13.4
33	"	"	"	(Run 33 omitted)		6.7
34	"	"	"	91.5	100	13.4
35	"	"	"	137.	100	6.7

Table 4.2 (continued). 1:650 Model Test Program--Concentrations

Run	Wind Direction (deg. az.)	Units Present	Units Operating	Stack Heights (m)	Operating Level (%)	Wind Velocity (m/s)
36	180	1C,1-8	1C,6,7,8	137	100	13.4
37	"	"	"	183.	100	6.7
38	"	"	"	"	"	13.4
39	243	1,2,3,4,5	1,2,3,4,5	45. (1,2,3,4) 91.5 (5)	100	6.7
40	"	"	"	"	"	13.4
41	"	"	"	"	75	6.7
42	"	"	"	"	"	13.4
43	"	1C,1-4,5,6,7,8	1C,6,7,8	91.5	100	6.7
44	"	"	"	"	"	13.4
45	"	"	"	"	75	6.7
46	"	"	"	"	"	13.4
47	"	"	"	137.	100	6.7
48	"	"	"	"	"	13.4
49	"	"	"	183.	100	6.7
50	"	"	"	"	"	13.4
51	333	1,2,3,4,5	1,2,3,4,5	45. (1,2,3,4) 91.5 (5)	100	6.7
52	"	"	"	"	"	13.4
53	"	"	"	"	"	6.7
54	"	"	"	"	"	13.4
55	"	1C,1-4,5,6,7,8	1C,6,7,8	91.5	100	6.7
56	"	"	"	"	"	13.4
57	"	"	"	"	"	6.7
58	"	"	"	"	"	13.4
59	"	"	"	137.	100	6.7
60	"	"	"	"	"	13.4
61	"	"	"	183.	100	6.7
62	"	"	"	"	"	13.4
63	0	1,2,3,4,5	1,2,3,4,5	45. (1,2,3,4) 91.5 (5)	100	6.7
64	"	"	"	"	"	13.4
65	"	"	"	"	75	6.7
66	"	"	"	"	"	13.4
67	"	1C,1-4,5,6,7,8	1C,6,7,8	91.5	100	6.7
68	"	"	"	"	"	13.4
69	"	"	"	"	75	6.7
70	"	"	"	"	"	13.4
71	"	"	"	137.	100	6.7
72	"	"	"	"	"	13.4
73	"	"	"	183.	100	6.7
74	"	"	"	"	"	13.4